Supplementary Material for

Absolute plate motions since 130 Ma constrained by subduction zone kinematics

Simon Williams, Nicolas Flament, R. Dietmar Müller, Nathaniel Butterworth

Earth and Planetary Science Letters (doi:10.1016/j.epsl.2015.02.026)

A. Sensitivity of the global subduction zone characteristics to the uncertainty in the subduction history within the relative plate motion model

Aside from the APM models themselves, the factors contributing to uncertainty in trench migration are the timing and location of subduction, the relative plate motions, choice of temporal resolution for plate velocities and arc deformation.

1. Uncertainty in timing and location of subduction: Using APM model O2005, we modify the subduction history east of Australia from 130-50 Ma (Figure S2). A number of contrasting models exist for the Cretaceous to early Cenozoic tectonic evolution of this region; in terms of the timing of cessation of the long-lived Mesozoic subduction that preceded Tasman Sea spreading, and the history and polarity of subduction east of the Lord Howe Rise once spreading was underway in the Tasman Sea (Crawford et al., 2003; Sdrolias et al., 2003; Steinberger et al., 2004; Schellart et al., 2006; Sutherland et al., 2010; Matthews et al., 2015). The Seton et al. (2012) RPM model features west-dipping subduction in the early Cretaceous, followed by a switch to east-dipping subduction in the Late Cretaceous that continues until 50 Ma. Within the Seton et al. (2012) RPM model, this subduction zone extends for 5000-5500 km (the exact length varying through time), constituting ~8-9% of the total trench length. For the purposes of this sensitivity test, we tested two alternative scenarios – one where these subduction zones existed with the opposite polarity (b), and a second where these subduction zones were no longer present and thus do not contribute to the global statistics (c)(all other aspects of the plate kinematic model remain unchanged). Some aspects of these scenarios are unlikely to be realistic, but serve the purpose of illustrating the degree to the ill-defined tectonic history of a single region may skew our observations. The results in the first panel (a) are the reference case, and are same as those shown for APM model O2005 in the main text, while (b) and (c) are the global statistics for the two alternative subduction scenarios. The right column shows residuals between these two scenarios and the reference case, plotted with the same colour scale. The results indicate that first-order trends in the trench migration distributions are relatively insensitive to uncertainties in the history of regional subduction histories.

2. Uncertainty in relative plate motions: Taking the Andean margin as an example, the uncertainty on trench migration related to relative motions depends on the spreading history of the South Atlantic (South America relative to Africa), which is constrained by magnetic anomalies and fracture zones. Similar uncertainties exist for the motion of North America and Antarctica relative to Africa. For plates distant from Africa, relative plate motion uncertainty is the sum of uncertainties for each plate pair (for example the uncertainty in the motion of the trench along the Lord Howe Rise relative to the African plate depends on combined uncertainties in the relative motions of Africa-Antarctica, Antarctica-Australia and Australia-Lord Howe Rise rotations). Formal uncertainties in the rates of relative motion between plate pairs derived from the seafloor spreading record are calculated for many of the plate pairs used in the global model (e.g. Gaina et al., 1998). Uncertainty values are typically in the range 1-5 mm/yr (for full spreading rates).

3. Uncertainty related to temporal resolution used to calculate trench migration rates: The Seton et al. (2012) RPM model allows us to compute plate kinematic parameters at 1 Myr intervals, but we may expect the computed trench migration rates to be systematically lower if the plate velocities are averaged over longer time periods. In Figure S3 we compare the results of computing trench migration rates for the O2005 APM model, with plate kinematics averaged over 1, 5 and 10 Myr. The difference between the results is minor, reflecting the fact that the relative rotations contained within the Seton et al. (2012) RPM model are defined at relatively coarse time intervals compared to many detailed studies of seafloor spreading. The RPM model finite poles of rotation for the major plates are typically 5-10 Myr apart (Seton et al., 2012), so that it does not contain the high frequency noise known to occur in finite rotation poles when plate motion changes are defined at 1-2 Myr intervals (e.g. Iaffaldano et al., 2012).

4. Uncertainty related to arc deformation: To assess the effect of neglecting deformation affecting the shape and migration rate of the trench, we use the South American margin as a case study. Over the last 130 Ma, the most intense documented deformation is the shortening that has resulted in the Andean orocline. Recent studies suggest that major shortening and bending of the trench has taken place from <70 Ma to present day, with the maximum shortening during this time estimated at around 500 km (Kley, 1999; McQuarrie, 2002). Using these values as a proxy for the overall eastwards migration of the trench relative to ‘rigid’ South America (McQuarrie, 2002) suggests that the uncertainty in trench migration rate could be as much as 10 mm/yr where the shortening is most intense.

B. Comparison between observed seamount trails and predictions of APM and hotspot locations

We confine our analysis to the last 70 Ma, where constraints from hotspot trails are relatively abundant across multiple plates. Figure 6 of the main text show predicted hotspot trails using our base RPM model (Seton et al., 2012), and the candidate hotspot trail models for selected APM models. Results are plotted for the Tristan-Gough and Réunion trails, used in all four studies, and for the Hawaii-Emperor and Louisville trails, used in global studies. We omit the New England trail, since dated samples along this seamount chain are all older than 70 Ma. We include the Tasman Sea trails, that although not considered to be linked to deep plumes and rarely used to constrain APM models, are considered to be reliable indicators of the fast northward motion of the Australian plate in the past >25 Ma (McDougall and Duncan, 1988).

The dated samples we have used along each trail are taken from the existing compilations of dates for each trail within literature, including: McDougall and Duncan (1988) for the Tasmantid trail; O'Neill et al. (2005) for the St Helena trail; Doubrovine et al. (2012) for the Tristan-Gough and Réunion trails; and Wessel and Kroenke (2008), supplemented with more recent dates from Koppers et al. (2012) and O'Connor et al. (2013), for Pacific Trails. The present-day locations of hot spots are based on the compilation of Doubrovine et al. (2012) for all except the Tasmantid trail, for which we used a location based on Knesel et al. (2008).

Attempts to objectively compare the predictions of different hotspots APM models are complicated by the subtly different ways each APM model is constructed. For example, different models use different relative rotation parameters to link observations on different plates. APM models derived using moving hotspots are difficult to assess in a self-consistent manner where hotspot motions are not readily available. Moving hotspot models would typically be expected to produce a good fit to observations, compared to the fits for APM models where no hotspot motions have been inferred. In Figure 6, we limit the plotted trails to three cases that can be illustrated self-consistently: we plot the predicted trails of fixed hotspot APM model M1993 using the Seton et al. (2012) RPM model, hotspot trails predicted by APM model D2012 using their own rotation parameters for the motions of both the plates and individual hotspots, and predictions of the V2010 model using the Seton et al. (2012) RPM model and a fixed hotspot approximation. Note that model D2012 differs from other trails both due to the incorporation of hotspot motion, and the use of an alternative plate circuit to link the

Atlantic and Pacific domains prior to ~45 Ma. Both of these factors contribute to the better match observed for model D2012 for the Hawaii trail compared to other APM model predictions. Model V2010 poorly matches the trend of trails that lie either entirely or predominantly on the African plate.

Supplementary References

Crawford, A., Meffre, S., and Symonds, P., 2003, 120 to 0 Ma tectonic evolution of the southwest Pacific and analogous geological evolution of the 600 to 220 Ma Tasman Fold Belt System: Geological Society of America Special Papers, v. 372, p. 383-403.

Doubrovine, P.V., Steinberger, B., and Torsvik, T.H., 2012, Absolute plate motions in a reference frame defined by moving hot spots in the Pacific, Atlantic, and Indian oceans: Journal of Geophysical Research, v. 117, p. B09101.

Iaffaldano, G., Bodin, T., and Sambridge, M., 2012, Reconstructing plate-motion changes in the presence of finite-rotations noise: Nature Communications, v. 3, p. 1048.

Kley, J., 1999, Geologic and geometric constraints on a kinematic model of the Bolivian orocline: Journal of South American Earth Sciences, v. 12, p. 221-235.

Knesel, K.M., Cohen, B.E., Vasconcelos, P.M., and Thiede, D.S., 2008, Rapid change in drift of the Australian plate records collision with Ontong Java plateau: Nature, v. 454, p. 754-757.

Koppers, A.A., Yamazaki, T., Geldmacher, J.r., Gee, J.S., Pressling, N., Hoshi, H., Anderson, L., Beier, C., Buchs, D., and Chen, L., 2012, Limited latitudinal mantle plume motion for the Louisville hotspot: Nature Geoscience, v. 5, p. 911-917.

Matthews, K.J., Williams, S.E., Whittaker, J.M., Müller, R.D., Seton, M., and Clarke, G.L., 2015, Geologic and kinematic constraints on Late Cretaceous to mid Eocene plate boundaries in the southwest Pacific: Earth-Science Reviews, v. 140, p. 72-107.

McDougall, I., and Duncan, R.A., 1988, Age progressive volcanism in the Tasmantid Seamounts: Earth and Planetary Science Letters, v. 89, p. 207-220.

McQuarrie, N., 2002, Initial plate geometry, shortening variations, and evolution of the Bolivian orocline: Geology, v. 30, p. 867-870.

O'Connor, J.M., Steinberger, B., Regelous, M., Koppers, A.A., Wijbrans, J.R., Haase, K.M., Stoffers, P., Jokat, W., and Garbe-Sch__onberg, D., 2013, Constraints on past plate and mantle motion from new ages for the Hawaiian-Emperor Seamount Chain: Geochemistry, Geophysics, Geosystems, v. 14, p. 4564-4584.

O'Neill, C., Müller, D., and Steinberger, B., 2005, On the uncertainties in hot spot reconstructions and the significance of moving hot spot reference frames: Geochem. Geophys. Geosyst, v. 6, p. Q04003.

Schellart, W., Lister, G., and Toy, V., 2006, A Late Cretaceous and Cenozoic reconstruction of the Southwest Pacific region: tectonics controlled by subduction and slab rollback processes: Earth-Science Reviews, v. 76, p. 191-233.

Sdrolias, M., Müller, R., and Gaina, C., 2003, Tectonic evolution of the southwest Pacific using constraints from backarc basins: Geological Society of America Special Papers, v. 372, p. 343-359.

Seton, M., Müller, R., Zahirovic, S., Gaina, C., Torsvik, T., Shephard, G., Talsma, A., Gurnis, M., Turner, M., and Maus, S., 2012, Global continental and ocean basin reconstructions since 200Ma: Earth-Science Reviews, v. 113, p. 212-270.

Steinberger, B., Sutherland, R., and O'connell, R.J., 2004, Prediction of Emperor-Hawaii seamount locations from a revised model of global plate motion and mantle flow: Nature, v. 430, p. 167-173.

Sutherland, R., Collot, J., Lafoy, Y., Logan, G.A., Hackney, R., Stagpoole, V., Uruski, C., Hashimoto, T., Higgins, K., and Herzer, R.H., 2010, Lithosphere delamination with foundering of lower crust and mantle caused permanent subsidence of New Caledonia Trough and transient uplift of Lord Howe Rise during Eocene and Oligocene initiation of Tonga-Kermadec subduction, western Pacific: Tectonics, v. 29.

Wessel, P., and Kroenke, L.W., 2008, Pacific absolute plate motion since 145 Ma: An assessment of the fixed hot spot hypothesis: Journal of Geophysical Research: Solid Earth, v. 113.

Figure S1: Trench-orthogonal trench migration rates in 10 Myr intervals for the eight APM models considered in this study. The four APM models based on hotspot trails are shown in the left column, models based on paleomagnetism in the upper right; the remaining models are based respectively on slab remnant mapping, and removal of net rotation. Abbreviations: M1993 = Müller et al., 1993; O2005 = O'Neill et al., 2005; T2008 = Torsvik et al., 2008; D2012 = Doubrovine et al., 2012; S2005 = Schettino and Scotese, 2005; T2012 = Torsvik et al., 2012 (Running Mean); V2010 = van der Meer et al., 2010; NNR = No-Net-Rotation, this study. These example results are plotted at the midway point for each stage of Africa absolute motion defined within each of the APM models tested. In addition to the absolute trench kinematics, topological plate boundaries and absolute plate velocities for the plate interiors derived on a regular grid are shown (Seton et al., 2012). All parameters are calculated using *GPlates* (Boyden et al., 2011). For clarity, trench migration arrows are only plotted for a subset of the 1 degree segments used in the full analysis

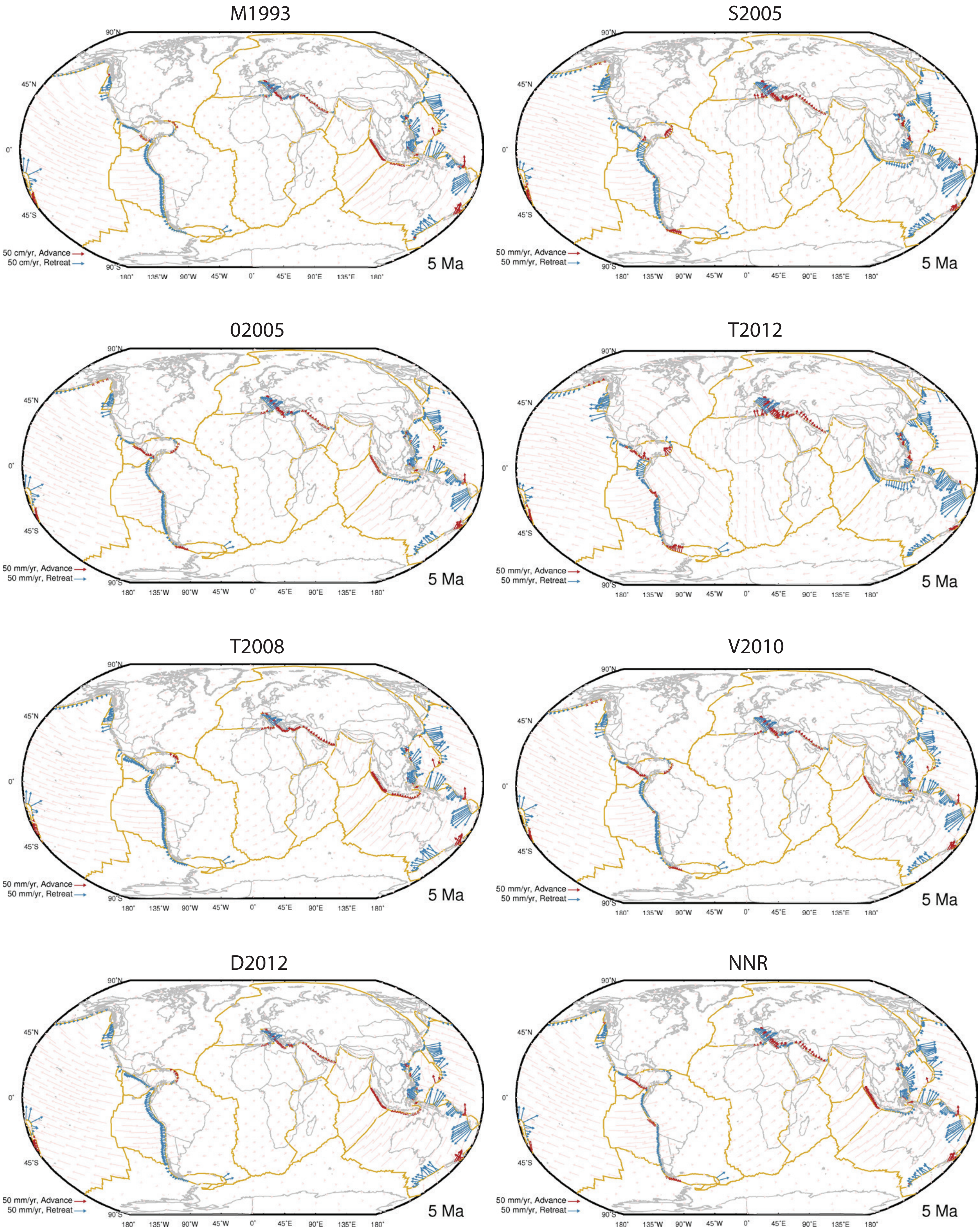
M1993
90°N
45°N
0°
45°S
90°S
180°
135°W
90°W
45°W
0°
45°E
90°E
135°E
180°
50 cm/yr, Advance
50 cm/yr, Retreat
5 Ma
S2005
50 mm/yr, Advance
50 mm/yr, Retreat
5 Ma
02005
50 mm/yr, Advance
50 mm/yr, Retreat
5 Ma
T2012
50 mm/yr, Advance
50 mm/yr, Retreat
5 Ma
T2008
50 mm/yr, Advance
50 mm/yr, Retreat
5 Ma
V2010
50 mm/yr, Advance
50 mm/yr, Retreat
5 Ma
D2012
50 mm/yr, Advance
50 mm/yr, Retreat
5 Ma
NNR
50 mm/yr, Advance
50 mm/yr, Retreat
5 Ma

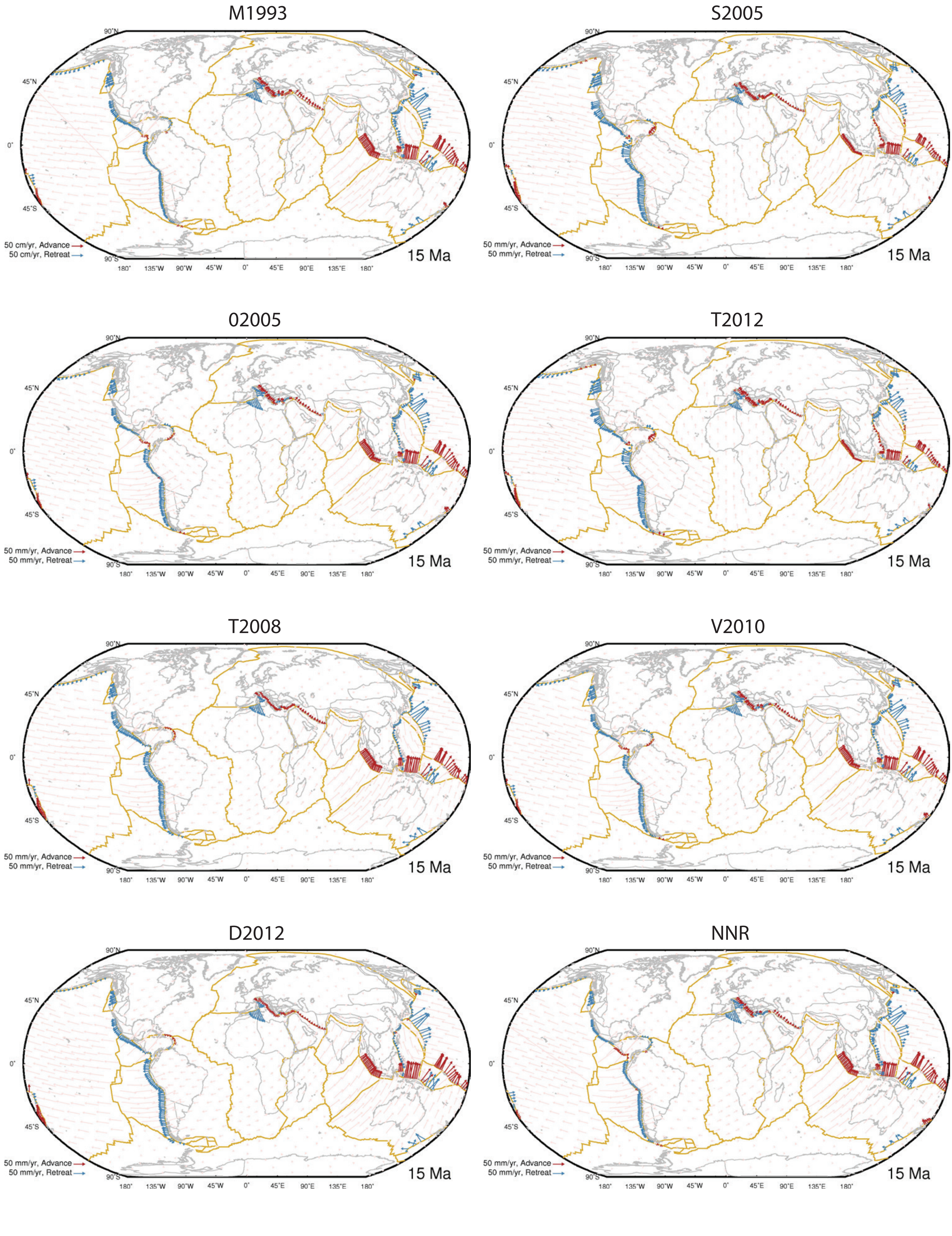
M1993
90°N
45°N
0°
45°S
90°S
50 cm/yr, Advance
50 cm/yr, Retreat
15 Ma
180° 135°W 90°W 45°W 0° 45°E 90°E 135°E 180°
S2005
90°N
45°N
0°
45°S
90°S
50 mm/yr, Advance
50 mm/yr, Retreat
15 Ma
180° 135°W 90°W 45°W 0° 45°E 90°E 135°E 180°
02005
90°N
45°N
0°
45°S
90°S
50 mm/yr, Advance
50 mm/yr, Retreat
15 Ma
180° 135°W 90°W 45°W 0° 45°E 90°E 135°E 180°
T2012
90°N
45°N
0°
45°S
90°S
50 mm/yr, Advance
50 mm/yr, Retreat
15 Ma
180° 135°W 90°W 45°W 0° 45°E 90°E 135°E 180°
T2008
90°N
45°N
0°
45°S
90°S
50 mm/yr, Advance
50 mm/yr, Retreat
15 Ma
180° 135°W 90°W 45°W 0° 45°E 90°E 135°E 180°
V2010
90°N
45°N
0°
45°S
90°S
50 mm/yr, Advance
50 mm/yr, Retreat
15 Ma
180° 135°W 90°W 45°W 0° 45°E 90°E 135°E 180°
D2012
90°N
45°N
0°
45°S
90°S
50 mm/yr, Advance
50 mm/yr, Retreat
15 Ma
180° 135°W 90°W 45°W 0° 45°E 90°E 135°E 180°
NNR
90°N
45°N
0°
45°S
90°S
50 mm/yr, Advance
50 mm/yr, Retreat
15 Ma
180° 135°W 90°W 45°W 0° 45°E 90°E 135°E 180°

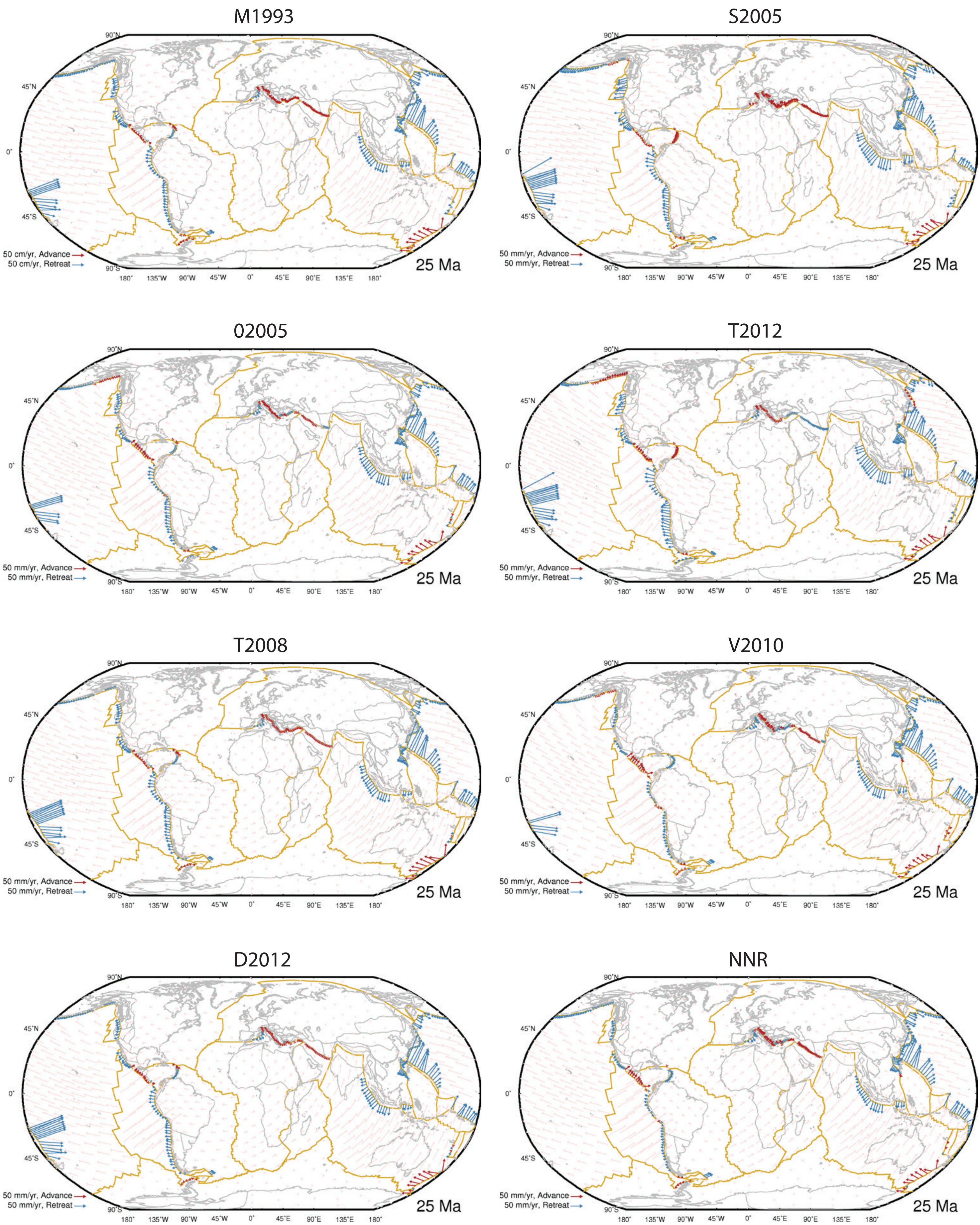
M1993
90°N
45°N
0°
45°S
90°S
50 cm/yr, Advance
50 cm/yr, Retreat
180°
135°W
90°W
45°W
0°
45°E
90°E
135°E
180°
25 Ma
S2005
50 mm/yr, Advance
50 mm/yr, Retreat
25 Ma
02005
50 mm/yr, Advance
50 mm/yr, Retreat
25 Ma
T2012
50 mm/yr, Advance
50 mm/yr, Retreat
25 Ma
T2008
50 mm/yr, Advance
50 mm/yr, Retreat
25 Ma
V2010
50 mm/yr, Advance
50 mm/yr, Retreat
25 Ma
D2012
50 mm/yr, Advance
50 mm/yr, Retreat
25 Ma
NNR
50 mm/yr, Advance
50 mm/yr, Retreat
25 Ma

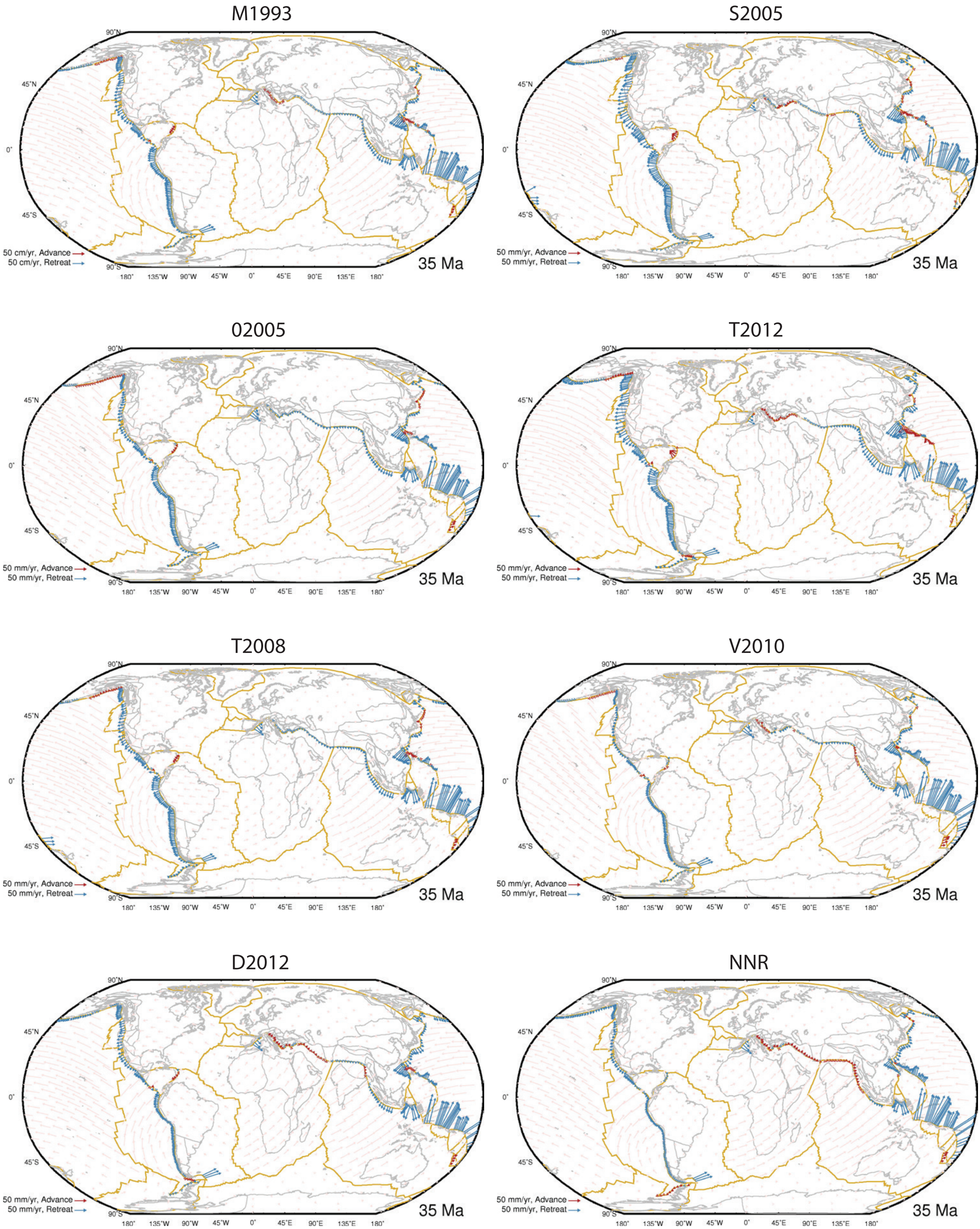
M1993
50 cm/yr, Advance
50 cm/yr, Retreat
35 Ma
S2005
50 mm/yr, Advance
50 mm/yr, Retreat
35 Ma
02005
50 mm/yr, Advance
50 mm/yr, Retreat
35 Ma
T2012
50 mm/yr, Advance
50 mm/yr, Retreat
35 Ma
T2008
50 mm/yr, Advance
50 mm/yr, Retreat
35 Ma
V2010
50 mm/yr, Advance
50 mm/yr, Retreat
35 Ma
D2012
50 mm/yr, Advance
50 mm/yr, Retreat
35 Ma
NNR
50 mm/yr, Advance
50 mm/yr, Retreat
35 Ma
90°N
45°N
0°
45°S
90°S
180°
135°W
90°W
45°W
45°E
90°E
135°E

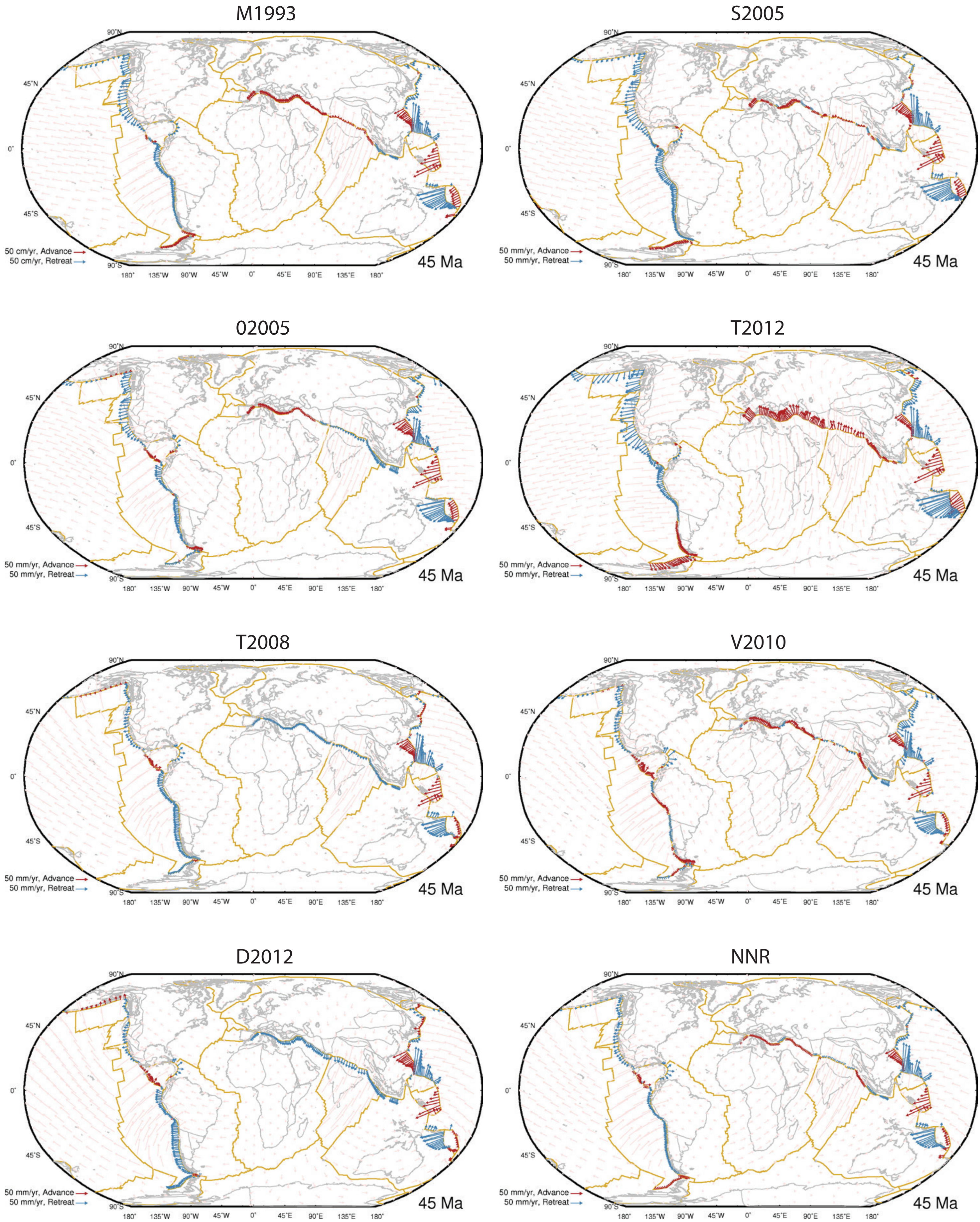
M1993
90°N
45°N
0°
45°S
90°S
50 cm/yr, Advance
50 cm/yr, Retreat
180°
135°W
90°W
45°W
0°
45°E
90°E
135°E
180°
45 Ma
S2005
90°N
45°N
0°
45°S
90°S
50 mm/yr, Advance
50 mm/yr, Retreat
180°
135°W
90°W
45°W
0°
45°E
90°E
135°E
180°
45 Ma
02005
90°N
45°N
0°
45°S
90°S
50 mm/yr, Advance
50 mm/yr, Retreat
180°
135°W
90°W
45°W
0°
45°E
90°E
135°E
180°
45 Ma
T2012
90°N
45°N
0°
45°S
90°S
50 mm/yr, Advance
50 mm/yr, Retreat
180°
135°W
90°W
45°W
0°
45°E
90°E
135°E
180°
45 Ma
T2008
90°N
45°N
0°
45°S
90°S
50 mm/yr, Advance
50 mm/yr, Retreat
180°
135°W
90°W
45°W
0°
45°E
90°E
135°E
180°
45 Ma
V2010
90°N
45°N
0°
45°S
90°S
50 mm/yr, Advance
50 mm/yr, Retreat
180°
135°W
90°W
45°W
0°
45°E
90°E
135°E
180°
45 Ma
D2012
90°N
45°N
0°
45°S
90°S
50 mm/yr, Advance
50 mm/yr, Retreat
180°
135°W
90°W
45°W
0°
45°E
90°E
135°E
180°
45 Ma
NNR
90°N
45°N
0°
45°S
90°S
50 mm/yr, Advance
50 mm/yr, Retreat
180°
135°W
90°W
45°W
0°
45°E
90°E
135°E
180°
45 Ma

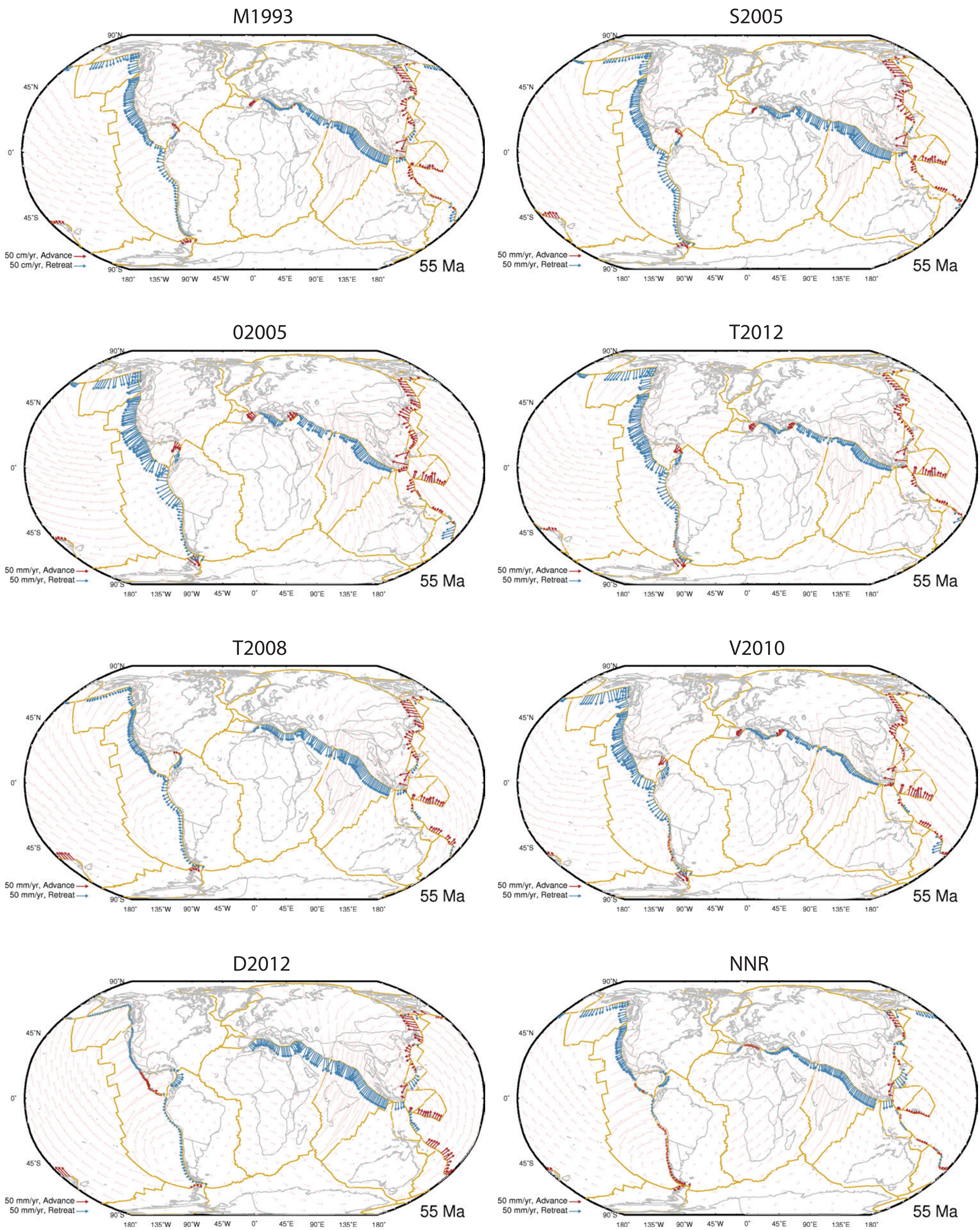

M1993
S2005
02005
T2012
T2008
V2010
D2012
NNR
90°N
45°N
0°
45°S
90°S
180°
135°W
90°W
45°W
0°
45°E
90°E
135°E
180°
50 cm/yr, Advance
50 cm/yr, Retreat
50 mm/yr, Advance
50 mm/yr, Retreat
55 Ma

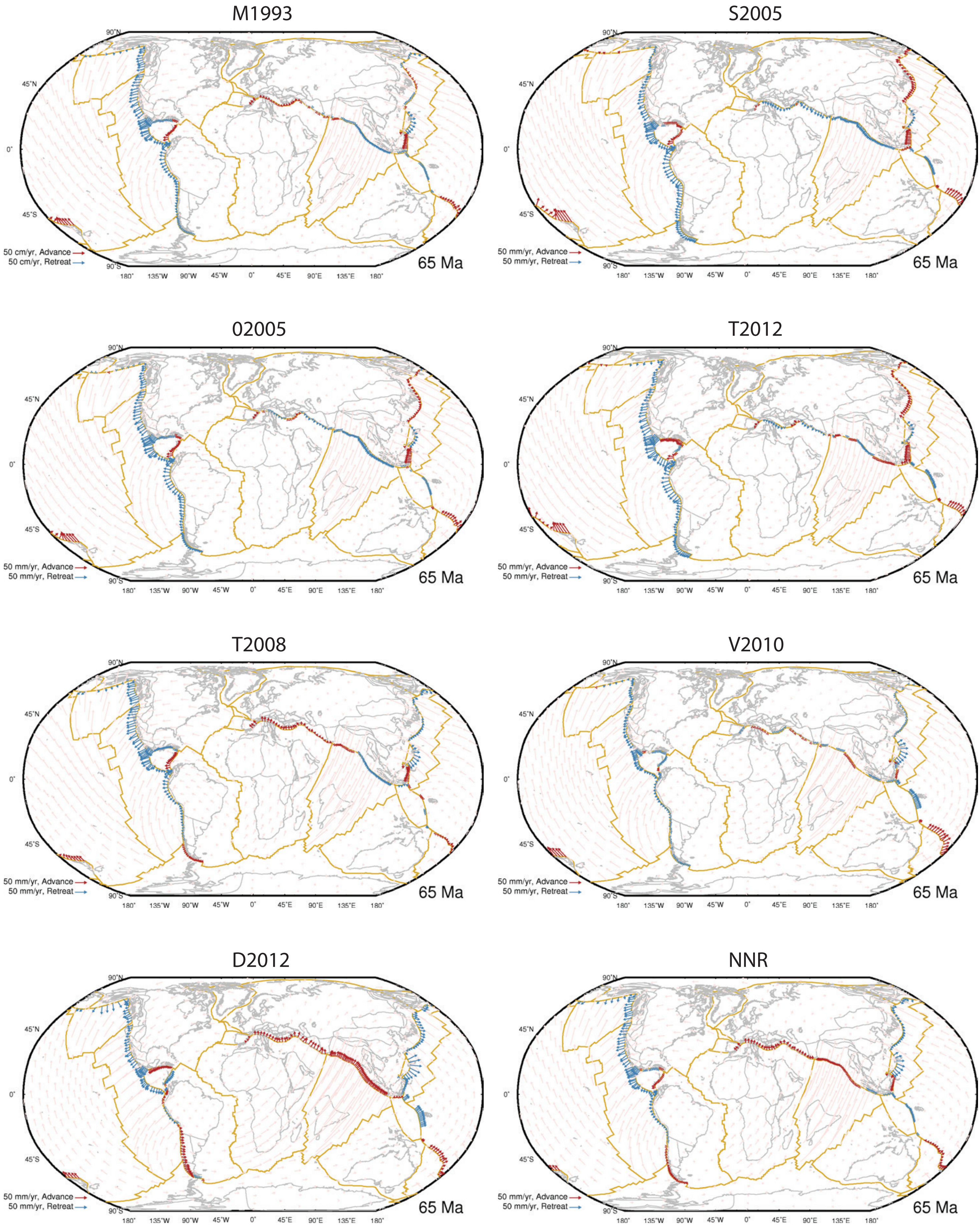
M1993
90°N
45°N
0°
45°S
90°S
180° 135°W 90°W 45°W 0° 45°E 90°E 135°E 180°
50 cm/yr, Advance
50 cm/yr, Retreat
65 Ma
S2005
90°N
45°N
0°
45°S
90°S
180° 135°W 90°W 45°W 0° 45°E 90°E 135°E 180°
50 mm/yr, Advance
50 mm/yr, Retreat
65 Ma
02005
90°N
45°N
0°
45°S
90°S
180° 135°W 90°W 45°W 0° 45°E 90°E 135°E 180°
50 mm/yr, Advance
50 mm/yr, Retreat
65 Ma
T2012
90°N
45°N
0°
45°S
90°S
180° 135°W 90°W 45°W 0° 45°E 90°E 135°E 180°
50 mm/yr, Advance
50 mm/yr, Retreat
65 Ma
T2008
90°N
45°N
0°
45°S
90°S
180° 135°W 90°W 45°W 0° 45°E 90°E 135°E 180°
50 mm/yr, Advance
50 mm/yr, Retreat
65 Ma
V2010
90°N
45°N
0°
45°S
90°S
180° 135°W 90°W 45°W 0° 45°E 90°E 135°E 180°
50 mm/yr, Advance
50 mm/yr, Retreat
65 Ma
D2012
90°N
45°N
0°
45°S
90°S
180° 135°W 90°W 45°W 0° 45°E 90°E 135°E 180°
50 mm/yr, Advance
50 mm/yr, Retreat
65 Ma
NNR
90°N
45°N
0°
45°S
90°S
180° 135°W 90°W 45°W 0° 45°E 90°E 135°E 180°
50 mm/yr, Advance
50 mm/yr, Retreat
65 Ma

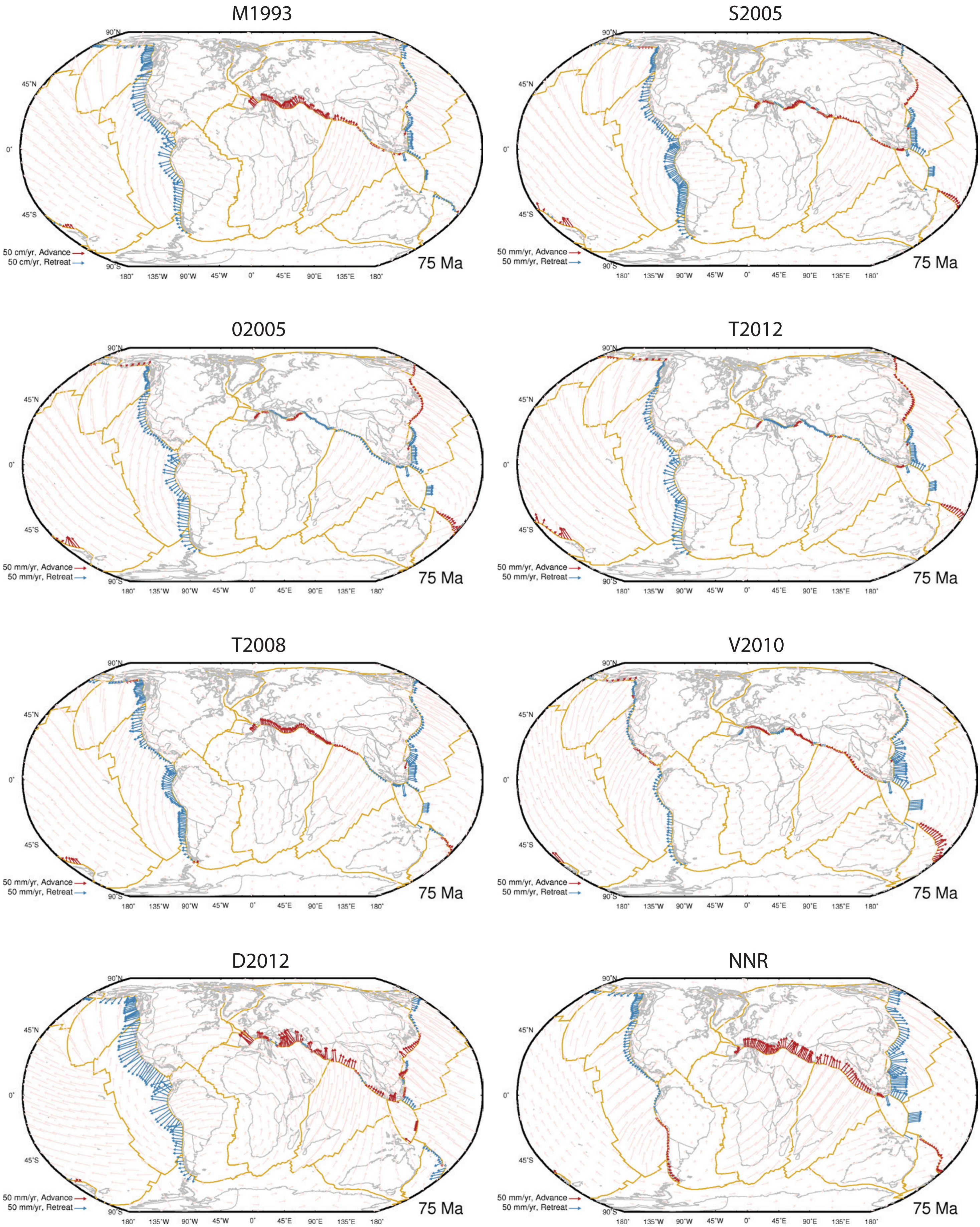
M1993
S2005
O2005
T2012
T2008
V2010
D2012
NNR
75 Ma
50 cm/yr, Advance
50 cm/yr, Retreat
50 mm/yr, Advance
50 mm/yr, Retreat
90°N
45°N
0°
45°S
90°S
180°
135°W
90°W
45°W
0°
45°E
90°E
135°E
180°

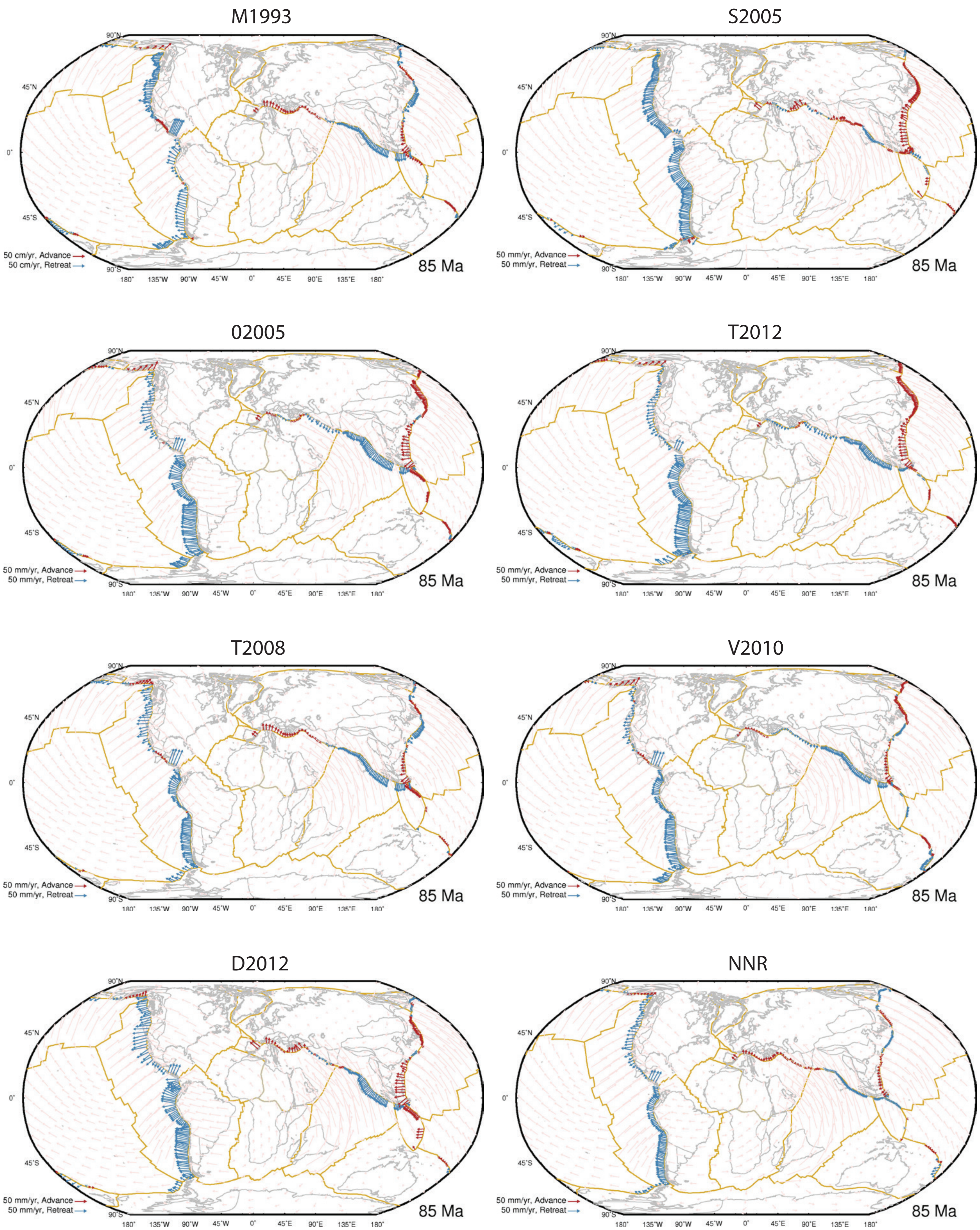
M1993
50 cm/yr, Advance
50 cm/yr, Retreat
85 Ma
S2005
50 mm/yr, Advance
50 mm/yr, Retreat
85 Ma
02005
50 mm/yr, Advance
50 mm/yr, Retreat
85 Ma
T2012
50 mm/yr, Advance
50 mm/yr, Retreat
85 Ma
T2008
50 mm/yr, Advance
50 mm/yr, Retreat
85 Ma
V2010
50 mm/yr, Advance
50 mm/yr, Retreat
85 Ma
D2012
50 mm/yr, Advance
50 mm/yr, Retreat
85 Ma
NNR
50 mm/yr, Advance
50 mm/yr, Retreat
85 Ma
90°N
45°N
0°
45°S
90°S
180°
135°W
90°W
45°W
0°
45°E
90°E
135°E
180°

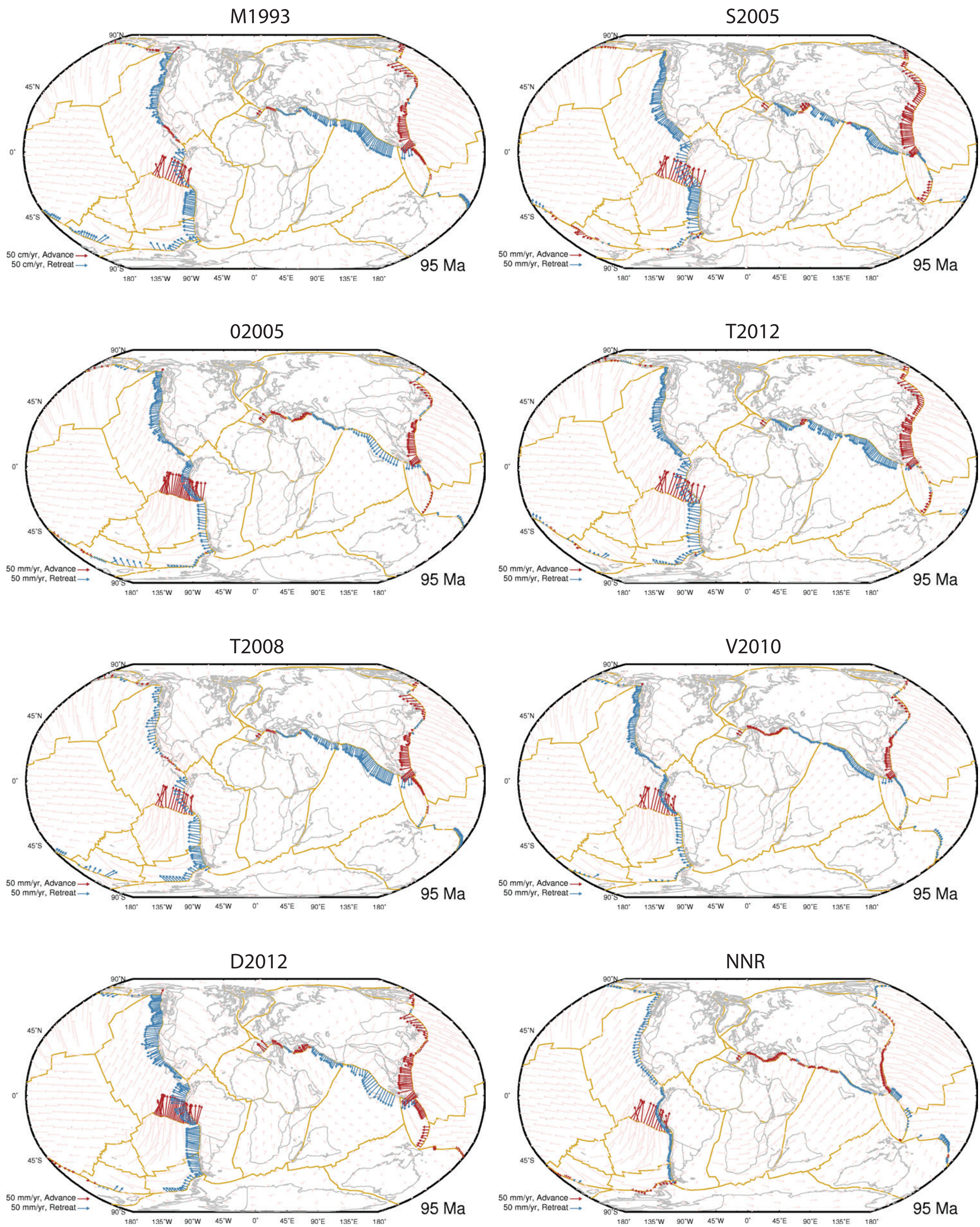
M1993
S2005
02005
T2012
T2008
V2010
D2012
NNR
90°N
45°N
0°
45°S
90°S
180°
135°W
90°W
45°W
0°
45°E
90°E
135°E
180°
50 cm/yr, Advance
50 cm/yr, Retreat
50 mm/yr, Advance
50 mm/yr, Retreat
95 Ma

M1993

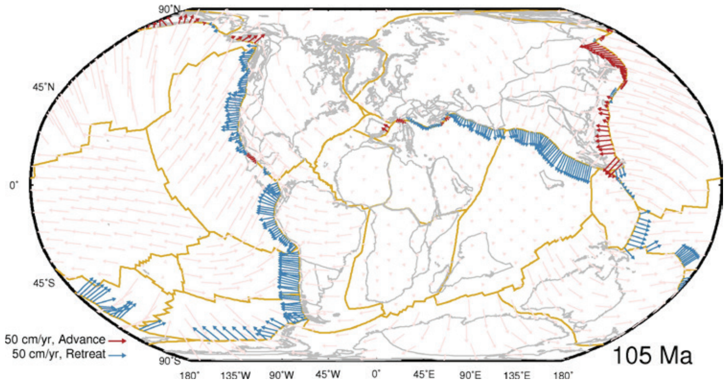

S2005

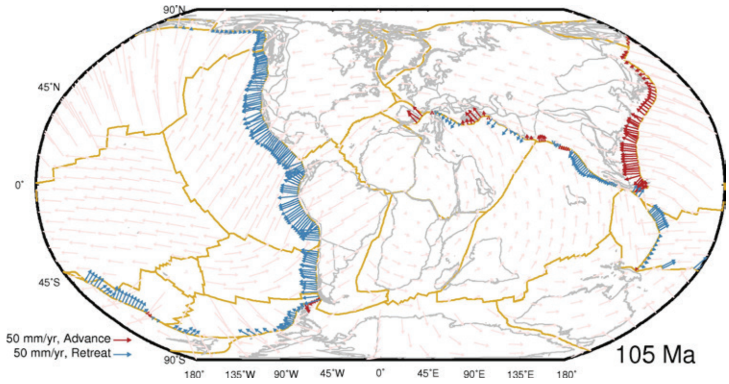

02005

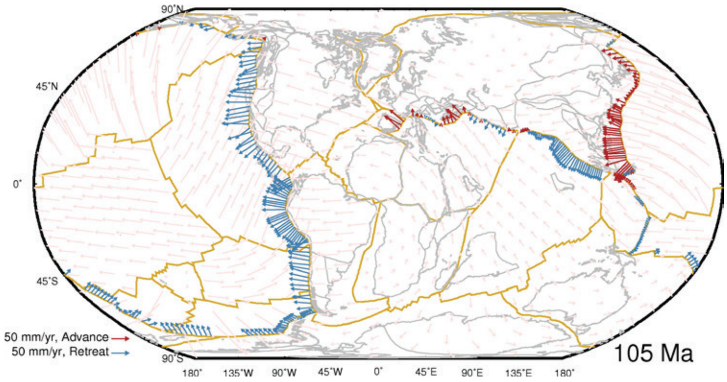

T2012

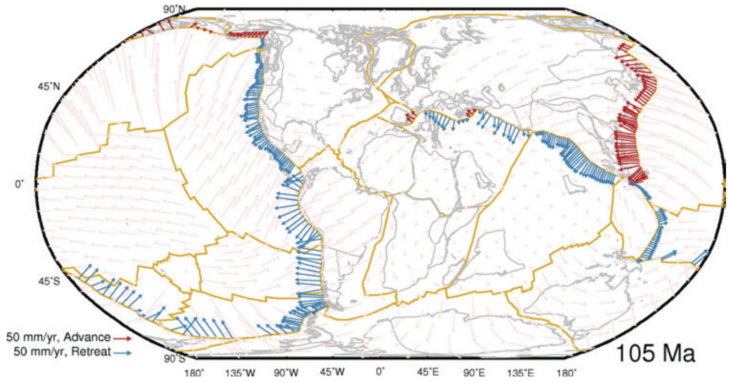

T2008

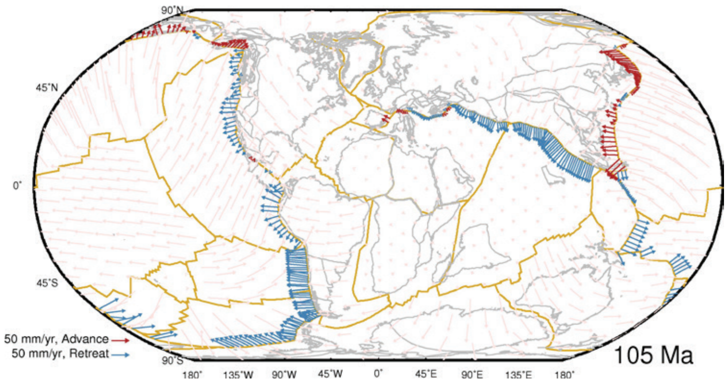

V2010

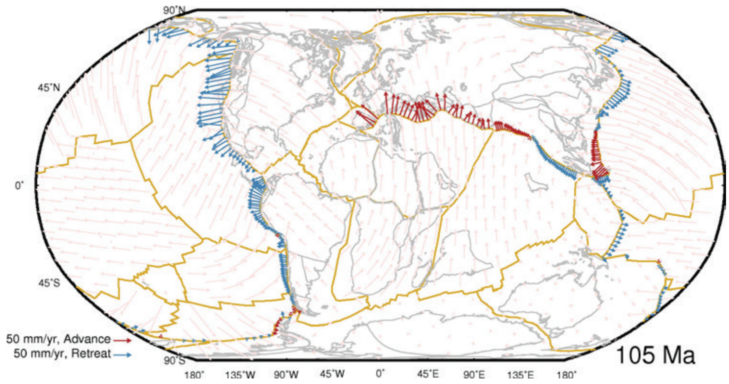

D2012

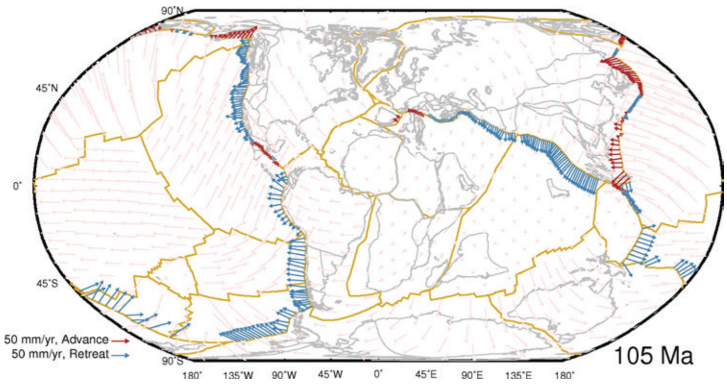

NNR

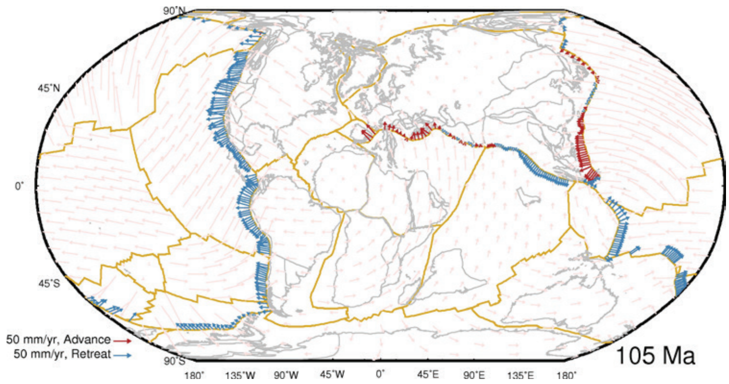

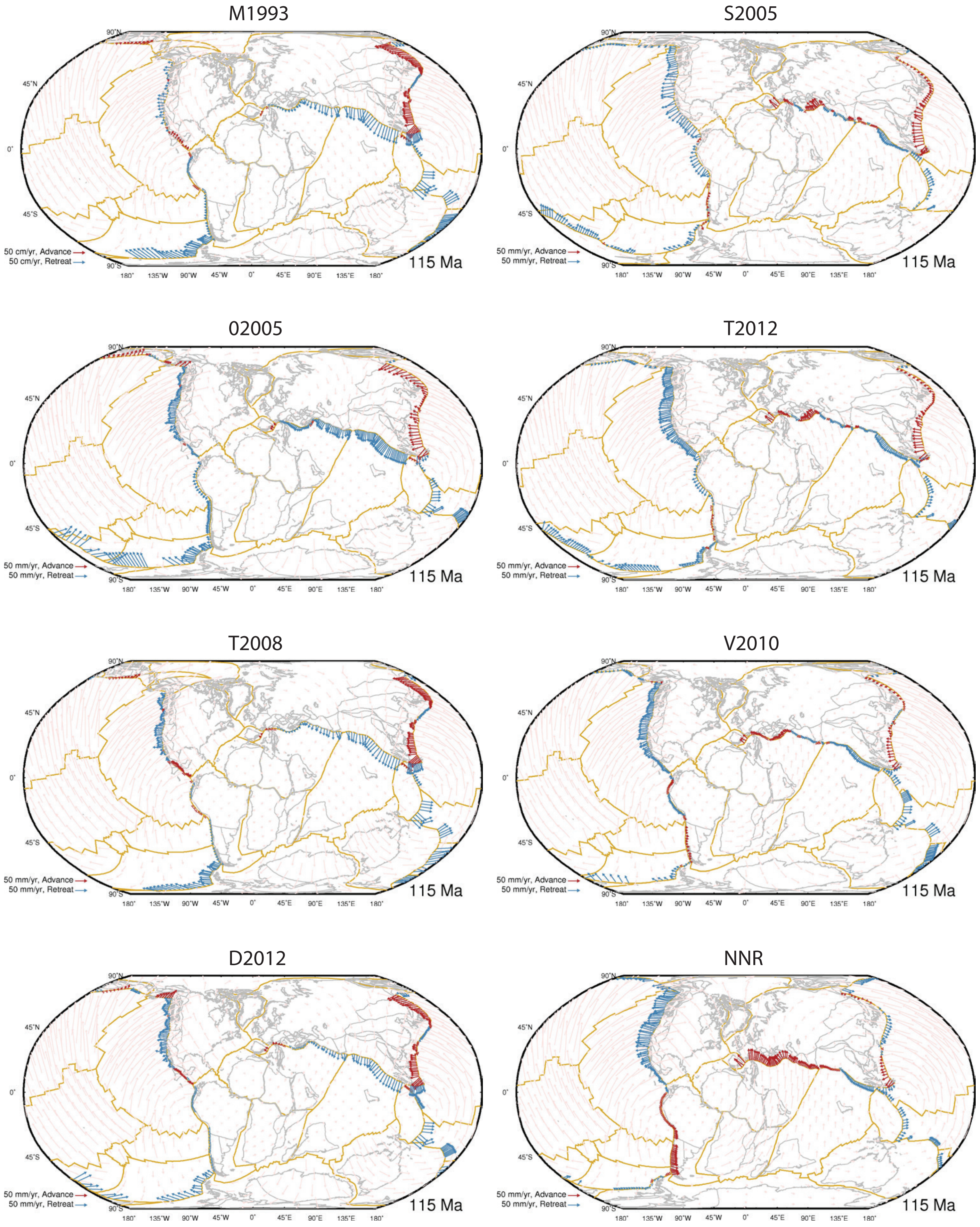

M1993
S2005
02005
T2012
T2008
V2010
D2012
NNR
90°N
45°N
0°
45°S
90°S
180°
135°W
90°W
45°W
0°
45°E
90°E
135°E
180°
50 cm/yr, Advance
50 cm/yr, Retreat
50 mm/yr, Advance
50 mm/yr, Retreat
115 Ma

M1993

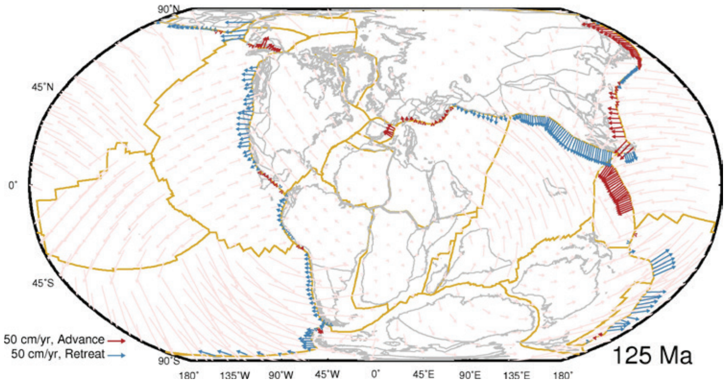

S2005

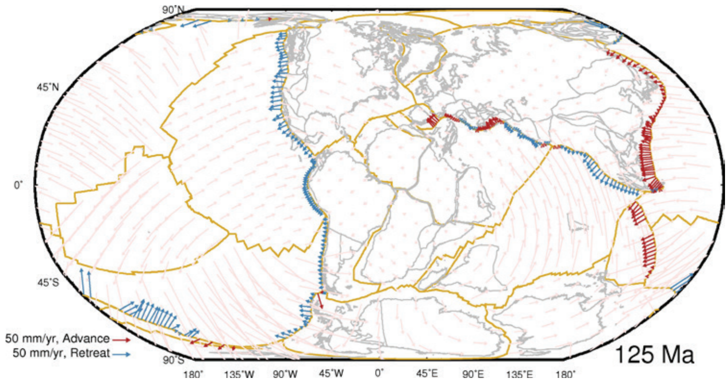

02005

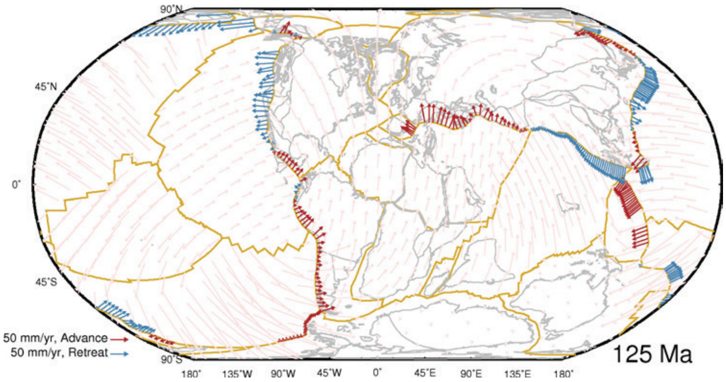

T2012

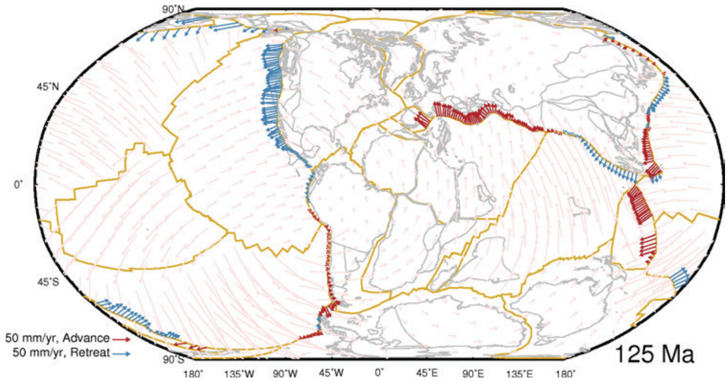

T2008

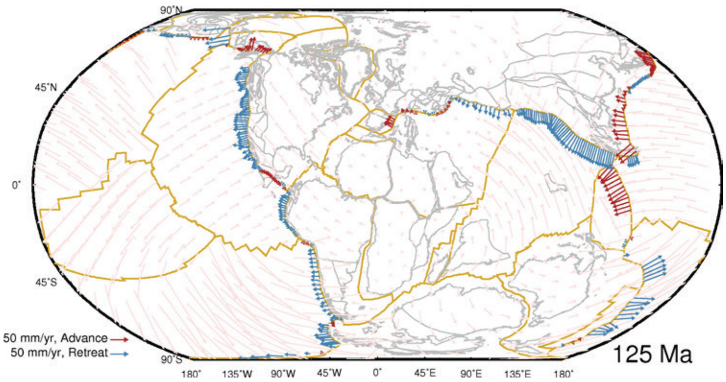

V2010

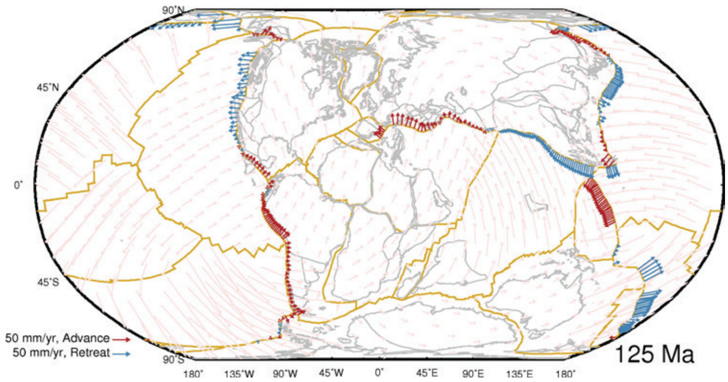

NNR

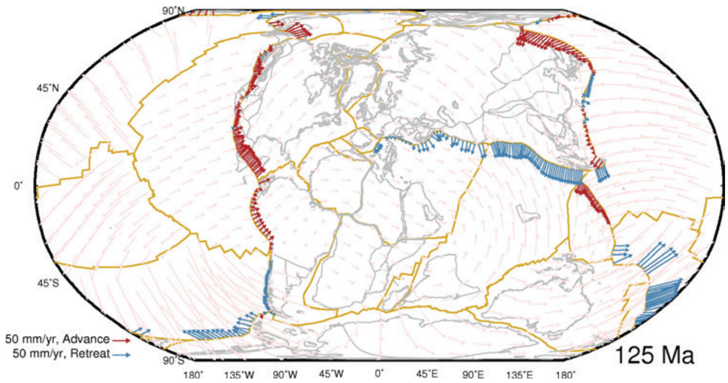

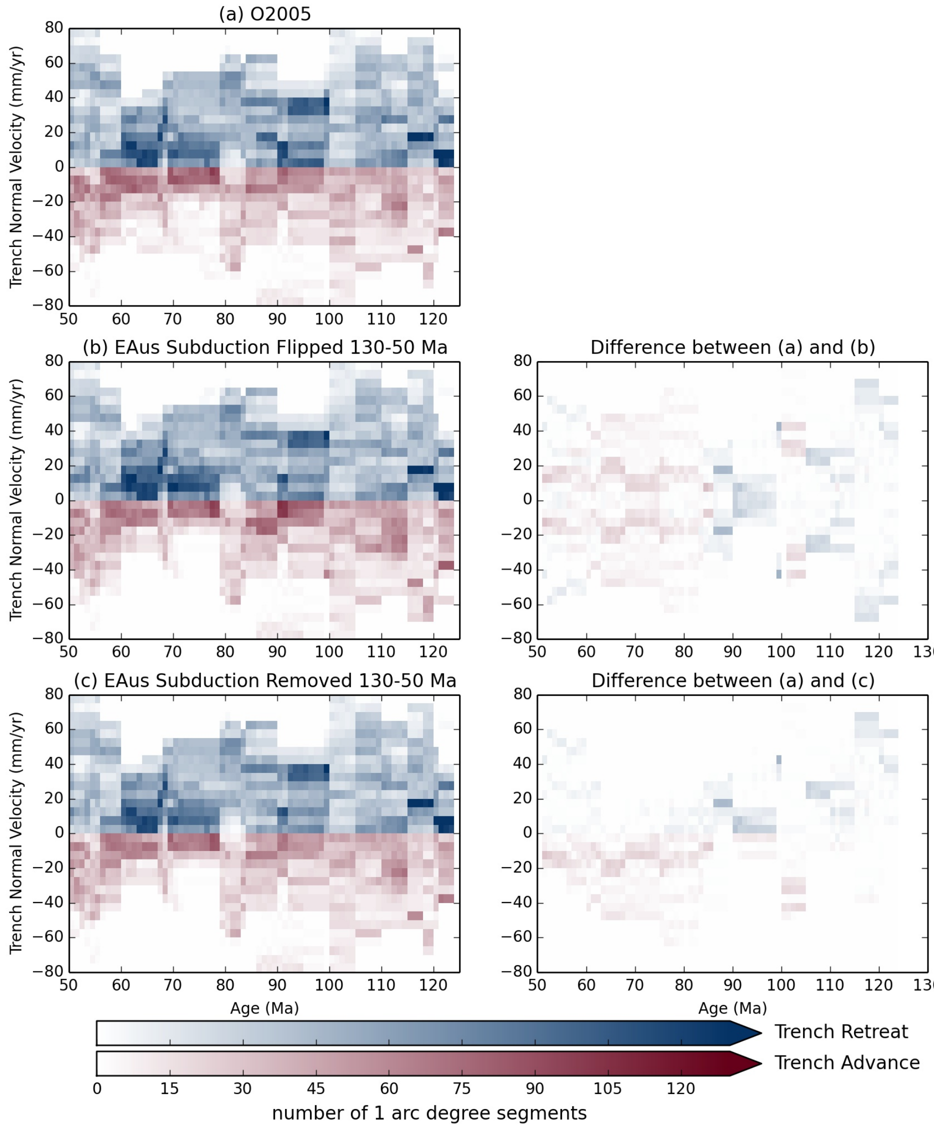

Figure S2: Sensitivity of results to uncertainty in subduction history. (a) global statistics for the reference case (based on APM model O2005) for 50-130 Ma; (b) global statistics computed for the same model as (a), but with the polarity of subduction along East Australia flipped; the right panel shows the difference between (a) and (b); (c) global statistics for a case where there is no subduction zone along Eastern Australia during this time period; the panel to the right shows the difference between cases (a) and (c).

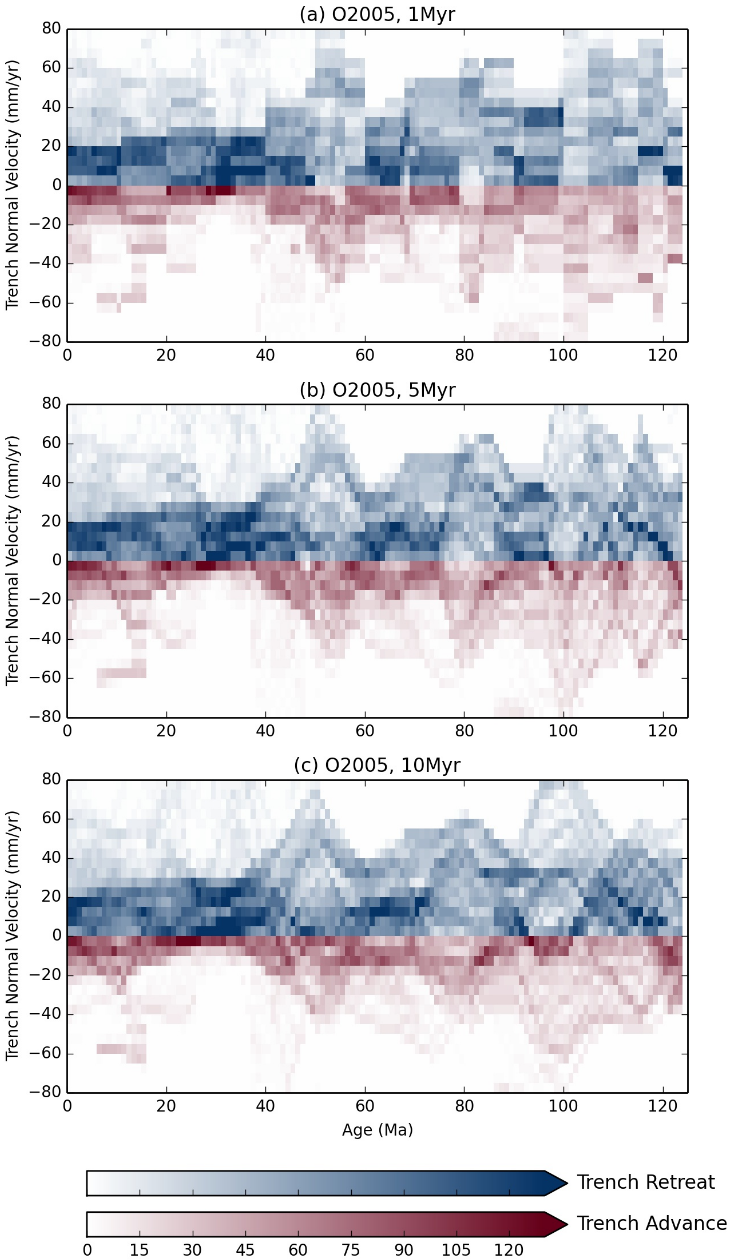

Figure S3: Influence of temporal resolution used to compute trench migration rates. In each case, the trench migration rates are calculated using the plate boundary configuration at a given time instant, but with all plate velocity values derived by averaging over different time range; (a) 1 Myr, (b) 5 Myr, and (c) 10 Myr.